is 1,2-propylenediamine). We thus find that (Figure 6) there is a strong increase in log K for a variety of metal ions as the σ^* values for these ligands increase, provided that they are symmetrically substituted. This at first sight seems inexplicable, unless we note that, while the σ^* values increase linearly from methylamine to *tert*-butylamine as more methyl groups are added, the E_s values "telescope", so that they are for methyl 0.00, ethyl 0.07, isopropyl 0.47, and *tert*-butyl 1.54. Thus, the symmetrical ligand DL-bn produces the same inductive strength as Me_2en (1,1-dimethylethylenediamine), because DL-bn is in our model composed of two ethyl groups, while Me_2en is composed of one methyl and one isopropyl. The latter ligand has, however, a much larger combined E_s value of 0.47, as against only 0.14 for the two ethyl groups of DL-bn. Figure 6 shows how finely balanced are the contributions of inductive and steric effects, in that such a seemingly small change as placing both methyl groups on the same C atom of the bridge of Me_2en can destabilize the complex relative to that of en, whereas placing them on separate C atoms as in DL-bn can stabilize the complex.

One of the important features of the macrocyclic effect is[8] that with N-donor macrocycles, provided that the metal ion fits reasonably well into the macrocycle, there is a strong increase in the ligand field parameter $10Dq$. We find that for *C*-methyl-substituted en ligands the same effect is found. Thus, in the square-planar form of the Ni(II) complex with en, the single intense transition occurs at 22 200 cm^{-1}, while in the analogous complex[6] with Me_4en the transition occurs at 23 000 cm^{-1}. Similarly, for the square-planar Ni(II) complexes of triethylenetetramine, this transition occurs at 22 300 cm^{-1}, while for the macrocycle 13-aneN_4 (1,4,7,10-tetraazacyclotridecane) it occurs[34] at 23 530 cm^{-1}. The similar response of the above ligand field transitions, and the "hidden" nature of the inductive effects, whether we are dealing with the effects of C-methylation on en type ligands, or the macrocyclic effect, suggests that the extra stabilizations observed for both these effects are in many ways similar in origin.

Conclusions. The binding of the proton to ligands in water is not always a good indicator of inductive effects, which therefore may be "hidden". Gas-phase results show up these hidden inductive effects very strongly, for both the proton and other Lewis acids. For both the proton and other Lewis acids, these inductive effects may be masked in aqueous solution by steric hindrance. For metal ions with low susceptibility to steric hindrance such as Ag(I) with primary amines or square-planar Cu(II) and Ni(II) with C-methylated en ligands, the inductive effects may be able to overcome steric effects and manifest themselves as increasing complex stability and stronger ligand fields.

Acknowledgment. The authors thank the Senate Research Committee of the University of the Witwatersrand and the Council for Scientific and Industrial Research for financial support of this work and a bursary to B.S.N.

Registry No. (Cyanomethyl)amine, 540-61-4; benzylamine, 100-46-9; 3-aminopentane, 616-24-0; diisopropylamine, 108-18-9; ethylamine, 75-04-7; isopropylamine, 75-31-0; *tert*-butylamine, 75-64-9; cyclopentylamine, 1003-03-8.

(34) Fabbrizzi, L. *J. Chem. Soc., Dalton Trans.* **1979**, 1857.

Contribution from Sandia National Laboratories, Albuquerque, New Mexico 87185

Metal Effects on Metalloporphyrins and on Their π–π Charge-Transfer Complexes with Aromatic Acceptors: Urohemin Complexes†

J. A. SHELNUTT

Received July 13, 1982

Metallouroporphyrins containing Cu(II), Ni(II), Fe(III), and Co(II) were investigated with absorption and resonance Raman spectroscopy. Systematic spectral changes are observed as the metal is varied. The spectral changes associated with metal substitution were found to be similar to changes observed for π–π complexation of the metalloporphyrins with phenanthrolines. Further, metal substitution systematically alters spectral changes that accompany π–π complexation of the metalloporphyrin with neutral aromatic acceptors. The spectral changes can be traced to the effects of the metal ion and the π–π interaction on the highest occupied $a_{2u}(\pi)$ orbital of the porphyrin. An interpretation based on arguments concerning the $a_{2u}(\pi)$ orbital leads to an explanation of the core-size dependence of several Raman marker lines of metalloporphyrins and also of the spin-state marker lines in hemes. Iron(III) uroporphyrin and its complexes with derivatives of phenanthroline are examined in detail. The binding constants for these complexes and the resulting spectral changes are strikingly similar to those for complexes with other metal porphyrins. Both copper uroporphyrin and iron(III) uroporphyrin complexes show a proportionality between the shifts in the core-size marker lines and the acceptor properties of a series of phenanthroline derivatives. Comparisons of other spectroscopic and equilibrium binding data suggest that urohemin, like copper uroporphyrin, forms charge-transfer complexes with the phenanthroline ring parallel to the porphyrin macrocycle.

Introduction

Metalloporphyrin complexes, as intermediates in reactions catalyzed by the metalloporphyrins, are central to the phenomenon of catalytic activation, and, in particular, the coordination chemistry of the metal ion has been extensively studied in this regard. The porphyrin ring too plays an essential role in the catalytic process. For example, the macrocycle provides a "surface" with specific steric properties that influence catalytic reactions. In addition, cis and trans effects on axial coordination at the metal affect ligand reactivity and have received considerable attention.[1-4] Among the cis effects

† This work performed at Sandia National Laboratories supported by the U.S. Department of Energy under Contract DD-AC04-76-DP00789.

(1) Buchler, J. W.; Kokish, W.; Smith, P. D. *Struct. Bonding (Berlin)* **1978**, *34*, 79.
(2) Antipas, A.; Buchler, J. W.; Gouterman, M.; Smith, P. D. *J. Am. Chem. Soc.* **1980**, *102*, 198.

0020-1669/83/1322-2535$01.50/0

are the effects of peripheral substitution. The electron-withdrawing ability of substituents influences ligand affinity and reactivity by transmission of electronic structure differences in the porphyrin ring to the axial ligand(s) via the metal–porphyrin interaction.[1-4]

Another possible means of controlling the charge density that is available in the porphyrin ring for transfer to a metal ligand is by formation of a $\pi-\pi$ complex between an aromatic donor or acceptor and the porphyrin moiety. Charge transfer from the porphyrin ring to an aromatic acceptor, for example, will decrease the ring's π-electron density that is available to be moved onto a π-acceptor axial ligand such as O_2. This kind of mechanism has been postulated[5] for protein control of ligand-binding affinity in hemoglobin and may be involved in the control of biological functions of some of the other heme proteins such as the peroxidases.[6] Association with a metalloporphyrin also affects the aromatic molecule and may change its reactivity.[7] Therefore, it is of interest to spectroscopically determine the structures of these molecular complexes in solution and to ascertain the changes in the electronic structure of the $\pi-\pi$ complexed metalloporphyrin.

In earlier studies, nickel(II) uroporphyrin I (NiURO), copper(II) uroporphyrin I (CuURO), and the free base of uroporphyrin III were found to form complexes in H_2O with a wide variety of neutral and charged heterocyclic aromatic compounds, such as pyridine (py), caffeine, viologen, and phenanthroline (phen).[8-11] The uroporphyrins are convenient to study in aqueous solvent because they are freely soluble and do not aggregate appreciably at the concentrations necessary for Raman and absorption measurements.[11,12] Uroporphyrin (isomer I) has alternating acetic and propionic acid side chains at the eight β-carbon positions of the pyrrole rings. Lack of appreçiable aggregation of metallouroporphyrins at high pH is a result of electrostatic repulsion of the ionized carboxylic acid groups.[12] In addition, the Cu(II) and Ni(II) ions in the porphyrin ring do not readily add axial ligands. Therefore, these metalloporphyrins were ideal for use in experiments to identify and investigate $\pi-\pi$ complexes.

For this purpose, complexes of CuURO with a large numebr of phenanthroline derivatives were examined with Raman difference spectroscpy (RDS) and absorption spectroscopy.[8,9] The shifts in the Raman lines of the metalloporphyrin that are a result of complex formation were measured, as were the equilibrium binding constants (from absorption difference measurements). The acceptor properties of the phenanthrolines correlated well with observed frequency shifts in a group of Raman lines.[8,9] Phenanthroline derivatives that are hindered from lying flat on the porphyrin ring are an exception. On the other hand, Raman line shifts for a phenanthroline derivative that has sterically hindered nitrogen lone pairs did correlate with acceptor properties. Consequently, the phenanthrolines clearly do not coordinate directly with the metal ion but form $\pi-\pi$ charge-transfer complexes with the phenanthroline ring parallel to that of the porphyrin.

With the catalytically more interesting iron(III) uroporphyrins, however, the partially filled d_π orbitals of the out-of-plane Fe should be available for stronger axial coordination. However, the results presented in this paper demonstrate for some addends (e.g., for the phenanthrolines) that the presence of Fe(III) has little effect on either the binding affinity or structure of the complex in aqueous solution.

The present study examines the properties of the iron(III) uroporphyrin I (FeURO) complexes is some detail with Raman difference spectroscopy and absorption spectroscopy. In addition, the urohemin results are compared with those for nickel(II), cobalt(II), copper(II), and free-base uroporphyrin complexes. The covalency of the metal–porphyrin bond varies within this group,[10,13] and it is anticipated that differences in the varying degree of π bonding of the metal to the porphyrin ring will specifically affect the $\pi-\pi$ interaction in the charge-transfer complex. The resulting differences in the Raman line shifts are used to obtain a more detailed picture of the relative importance of the forces holding the complex together. In addition, new information concerning the metal–porphyrin interaction and the ways it can be affected by electronic properties of the porphyrin is obtained.

Materials and Methods

Iron(III) uroporphyrin I chloride was obtained from Porphyrin Products. A high fluorescence background in the spectrum of this material obscured the Raman spectrum, although the absorption spectrum exhibited no extra bands. Column chromatogrpahy on Sephadex G-50-40 removed most of the fluorescence background, and a reasonably good Raman spectrum could be obtained for the high-frequency region (1280–1680 cm^{-1}) at 457.9-nm excitation. In contrast, Raman spectra of fluorescent magnesium and zinc metallouroporphyrins could not be obtained because of background scattering and the fact that they were bleached by irradiation.

The cobalt uroporphyrin was also purchased from Porphyrin Products as the cobalt(III) uroporphyrin I chloride. A large amount of green impurity with peaks at 599, 559, and 434 nm was removed by first equilibrating a Sephadex column with a dithionite solution in 0.1 M NaOH and then reducing the cobalt(III) porphyrin with dithionite before application to the column. The green impurity is eluted before the cobalt(II) uroporphyrin I (CoURO). The phenanthrolines were obtained commercially as before[9] and were used without further purification.

Typically, samples were prepared by dissolving Fe(URO)Cl in about 1 mL of 0.1 M NaOH to a high concentration. This solution was chromatographed with 0.1 M NaOH as an eluent. The middle fractions were collected and further diluted ($\approx$1:10) with a 0.1 M NaOH solution in distilled H_2O, in Tris-buffered H_2O, or in methanol to about 8×10^{-5} M for Raman spectra and to 2×10^{-5} M for absorption spectra. Absorption spectra were obtained on a Perkin-Elmer Model 330 spectrophotometer with matched 1-mm or 10-mm thermoelectrically cooled quartz cells.

Raman difference spectra[5,14] were obtained by placing the solution of metallouroporphyrin in both sides of the partitioned Raman cell and adding the solid phenanthroline to give either a saturated solution or a concentration of at least 10^{-2} M. The cell was then placed into the rotator. The spectra of the complex and of the metallouroporphyrin alone were obtained simultaneously on the RDS apparatus.[5,9,14] Calculation of the difference spectra was performed on a Hewlett-Packard 9845T computer after signal averaging up to 50 0.5-h scans of a 400-cm^{-1} region of the Raman spectra. During long data collection times, the samples were monitored for decomposition by periodically dumping single-scan Raman spectra. No changes were noted in the Raman spectra of single scans during signal averaging. In some instances, fast Fourier transforms were used to smooth the Raman spectra.

The spectrometer resolution was 2 cm^{-1}. The power of the argon ion laser was about 300–400 mW in a partially focused beam; the Raman cell is rotated at $\sim$6000 rpm. The errors in the frequency differences reported are no greater than $\pm$0.2 cm^{-1} for the FeURO complexes and are smaller ($\pm$0.1 cm^{-1}) for the other metalloporphyrins.

(3) Antipas, A.; Buchler, J. W.; Gouterman, M.; Smith, P. D. *J. Am. Chem. Soc.* **1978**, *100*, 3015.
(4) Caughey, W. S.; Barlow, C. H.; O'Keefe, D. H.; O'Toole, M. C. *Ann. N.Y. Acad. Sci.* **1973**, *206*, 296.
(5) Shelnutt, J. A.; Rousseau, D. L.; Friedman, J. M.; Simon, S. R. *Proc. Natl. Acad. Sci. U.S.A.* **1976**, *76*, 4409.
(6) Shelnutt, J. A.; Satterlee, J. D.; Erman, J. E. *J. Biol. Chem.* **1983**, *258*, 2168.
(7) Manassen, J. *Catal. Rev.—Sci. Eng.* **1974**, *9*, 223.
(8) Shelnutt, J. A. *J. Am. Chem. Soc.* **1981**, *103*, 4275.
(9) Shelnutt, J. A. *J. Phys. Chem.* **1983**, *87*, 605.
(10) Shelnutt, J. A. *J. Am. Chem. Soc.* **1983**, *105*, 774.
(11) Mauzerall, D. *Biochemistry* **1965**, *4*, 1801.
(12) Blumberg, W. E.; Peisach, J. *J. Biol. Chem.* **1965**, *240*, 870.
(13) Berezin, B. D. "Coordination Compounds of Porphyrins and Phthalocyanines"; Vopian, V. G., Translator; Wiley: Chichester, 1981.
(14) Shelnutt, J. A.; Rousseau, D. L.; Dethmers, J.. K.; Margoliash, E. *Proc. Natl. Acad. Sci. U.S.A.* **1979**, *76*, 3865.

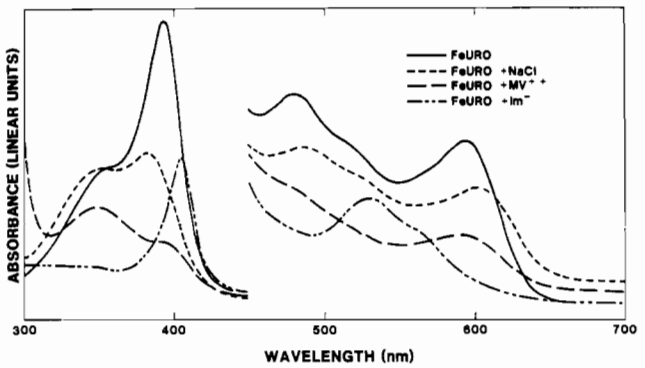

Figure 1. Absorption spectrum of iron(III) uroporphyrin in 0.1 M NaOH (—), the methylviologen (MV^{2+}) complex with FeURO (— —), the low-spin imidazole (Im) complex (— · · —) and salt-(NaCl) aggregated FeURO (- - -).

Results

Absorption Spectra and Spectral Changes. Copper uroporphyrin in either alkaline aqueous solution or aqueous methanol has a typical metalloporphyrin absorption spectrum with the α band at 562 nm, the β band at 524 nm, and the Soret band at 397 nm. The α and Soret bands correspond to $\pi-\pi^*$ transitions to the two lowest lying doubly degenerate electronic states of the macrocycle.[15] The β band is a vibrational sideband of the purely electronic transition to the lower of the two E_u states (D_{4h} molecular symmetry). Nickel and cobalt uroporphyrins also have typical metalloporphyrin absorption spectra, although their bands are hypsochromically shifted to 552 (α band), 516 (β band), and 392 nm (Soret) for Ni and to 551 nm (α band) with a shoulder at 520 nm (β band) and to 393 nm (Soret) for Co(II). The band maxima are close to those reported for the corresponding metalloctaethylporphyrins.[16]

In contrast, iron(III) uroporphyrin does not have a typical metalloporphyrin absorption spectrum (Figure 1) but exhibits "extra" bands thought to be the result of charge-transfer transitions involving the metal d orbitals.[3] The absorption spectrum of FeURO in 0.1 M NaOH solution (pH 14) in Figure 1 shows peaks at 593, 480, and 393 nm with clear shoulders at about 520 and 350 nm.

H_2URO has a typical[16] free-base porphyrin spectrum with four main peaks in the visible. The additional bands are results of reduced symmetry (D_{2h}) brought about by the protons on two of the pyrrollic nitrogens. The reduced symmetry splits the degeneracy of the α-band states and gives two purely electronic transitions of x and y polarization in the plane of the porphyrin ring—each with an associated vibrational satellite. The two bands of lowest energy at 600 and 559 nm are the x-polarized transition and its vibrational sideband.[17] (The N–H bonds are along the x axis.) The higher energy visible bands at 559, 537, and 501 nm and the somewhat broadened and asymmetric Soret at 396 nm have mixed x and y polarizations.[17]

Addition of other molecules to solutions of CuURO, CoURO, NiURO, Fe^{III}URO, and H_2URO produces shifts in the absorption bands.[8-11] Addition of neutral aromatic heterocyclic compounds generally results in a bathochromic shift of the absorption bands. An example is the addition of phenanthroline to an FeURO solution, which causes a red shift of 3–5 nm in the absorption bands in the visible (593 nm → 597 nm; 480 nm → 483 nm) and in the Soret band (393 nm → 398 nm). Figure 2 shows changes in the absorption difference spectrum that result from addition of phenanthroline to a solution of Fe^{III}URO in 0.1 M NaOH. A red shift in the Soret band occurs upon formation of the FeURO–phen complex, and a clear isosbestic point is observed at 399 nm. The lack of an isosbestic point in the 330–350-nm region is a result of phenanthroline absorption in this region. The concentrations of phenanthroline in Figure 2 are determined from the absorption difference at 320 nm. In alkaline H_2O, scattering from undissolved phenanthroline particles at the highest concentrations and the tail of phenanthroline absorption obscure the isosbestic points in the visible bands because of background shifts. However, in aqueous alkaline methanol, the solubility of phenanthrolines is not a problem, and clear isosbestic points are revealed.

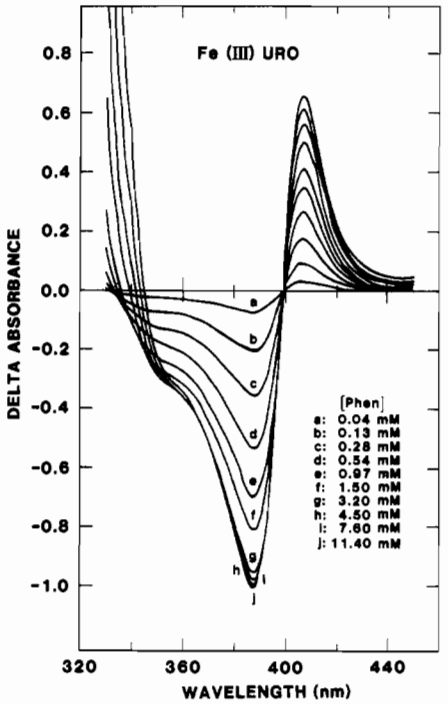

Figure 2. Absorption difference spectra of the Soret band of urohemin in 0.1 M NaOH at increasing concentrations of o-phenanthroline. The shape of the family of curves is indicative of a red shift in the Soret for the phen–FeURO complex.

For H_2URO, the addition of either phenanthroline or pyridine results in red shifts of all bands, but the shifts are considerably larger for the x-polarized bands than for the y-polarized ones.

The general rule that red shifts occur in the bands of the porphyrin upon complex formation has exceptions, however. For the imidazole–FeURO complex, the visible band shapes and positions change completely; a new band appears at 539 nm with a shoulder at 562 nm (Figure 1). The Soret band of the imidazole complex does show a bathochromic shift with disappearance of the shoulder at 350 nm. In contrast, the CuURO–imidazole complex is slightly bathochromically shifted in both visible and Soret regions.

The changes in the absorption spectrum of FeURO upon formation of complex with the methylviologen dication are shown in Figure 1. The viologen complex displays a blue shift and a broadening in the FeURO band at 593 nm and a weakening of the other visible bands. The Soret is weaker, and the former shoulder on the Soret becomes a band with a maximum at about 350 nm. Similarly, for the CuURO–MV^{2+} complex, a blue shift and a broadening was observed in the 562-nm band. However, in the Soret only a weakened red-shifted band was observed. CuURO has no extra band near 350 nm.

At high salt concentrations both CuURO[12] and urohemin aggregate. Figure 1 shows the effect of high NaCl concen-

(15) Gouterman, M. *J. Chem. Phys.* **1959**, *30*, 1139.
(16) Smith, K. M. "Porphyrins and Metalloporphyrins"; Elsevier: Amsterdam, 1975; p 884.

Table I. Equilibrium Binding Data for Metalloporphyrin Complexes at 27 °C

addend	solvent	MP	$10^5 \times$ [porphyrin], M	10^3[addend]$_{max}$, M (ΔA_{max})	ΔG, kcal/mol	% satn
1,10-phen	0.1 M NaOH	CuURO	1.8	6.5 (0.16)	5.3[a]	83
		FeURO	2.6	11.4 (1.7)	4.4	95
		H_2URO	28.0	1.5 (0.16)	3.5	86
	MeOH	CuURO	1.7	32 (0.18)	3.7	80
		NiURO	1.8	34.7 (0.28)	3.3	80
1,7-phen	0.1 M NaOH	CuURO	1.9	5.6 (0.18)	5.8[a]	93
	MeOH	CuURO	1.6	50 (0.16)	1.3	35
4,7-phen	0.1 M NaOH	CuURO	1.8	3.5 (0.16)	5.8	90
	MeOH	CuURO	1.1	50 (0.16)	1.8	35
2,9-Me_2phen	0.1 M NaOH	CuURO	1.9	2.6 (0.10)	4.5	82
		FeURO	1.7	1.8 (1.1)	4.5	76
	MeOH	CuURO	1.3	80 (0.21)	2.3	>70
4,7-Me_2phen	0.1 M NaOH	CuURO	1.9	4.5 (0.10)	4.3	82
	MeOH	CuURO	0.9	19.1 (0.17)	3.8	>85
5,6-Me_2phen	0.1 M NaOH	CuURO	1.9	3.5 (0.10)	4.4	80
	MeOH	CuURO	1.4	20 (0.30)	4.0	88
4-Me-phen	0.1 M NaOH	CuURO	1.9	12 (0.17)	5.3[a]	92
	MeOH	CuURO	2.6	77 (0.27)	3.8	93
5-Me-phen	0.1 M NaOH	CuURO	1.9	14 (0.17)	4.9[a]	86
5-Cl-phen	0.1 M NaOH	CuURO	1.8	5 (0.15)	6.2[a]	93
	MeOH	CuURO	1.3	39 (0.20)	4.2	95
5-NO_2phen	0.1 M NaOH	CuURO	1.9	6.0 (0.14)	4.1	87
5-Ph-phen	0.1 M NaOH	CuURO	1.9	3.9 (0.01)	4.1	27
	MeOH	CuURO	2.3	28.4 (0.06)	3.2	75
4,7-$(OH)_2$phen	0.1 M NaOH	CuURO	1.9	10 (0.06)	3.4	75
5,6-phen-dione	0.1 M NaOH	CuURO	2.0	29 (0.08)	2.8	73
MV^{2+}	0.1 M NaOH	CuURO	1.4	0.6 (0.09)	8.6	>98
pyridine	Tris (pH 8)	CuURO	1.1	1500 (0.40)	1.0	90
		H_2URO	7.9	2300 (0.07)	0.8	89
	0.1 M NaOH	FeURO	1.2	1500 (0.4)	0.8	80
		H_2URO	6.7	1400 (1.3)	0.7	80
2,6-lutidine	0.1 M NaOH	CuURO (23 °C)	1.3	1100	1.9	94
chloroquine	Tris (pH 8.4)	CuURO	1.2	2.5 (2.2)	6.3	>95
		FeURO	0.6	2.7 (1.2)	6.0	>95

[a] Result of a 2:1 binding analysis using a nonlinear, least-squares fitting routine.

trations on the absorption spectrum of FeURO. The Soret band of salt-aggregated FeURO is blue-shifted and reduced in intensity. The spectrum of the FeURO dimer is very similar to published Soret spectra of hematin in an aggregated state.[18-20] Neither CuURO nor the salt-induced CuURO dimer exhibits the strong shoulder in the 350-nm region evident in the urohemin spectra, but a large blue shift in the Soret is observed. The effect of salt on the absorption spectrum of NiURO is similar to its effect on solutions of CuURO.

At concentrations higher than those employed for the Raman and absorption measurements reported herein, aggregation of urohemin at pH 14 has been observed by using proton NMR.[21,22] Adding salt or lowering the temperature results in a shift in the dimer–monomer equilibrium in favor of the dimer. Only two forms are detected in the absorption spectrum.[22] Neither dimer nor monomer forms could be mistaken for μ-oxo dimer because the paramagnetic shifts are much larger than observed shifts for μ-oxo-dimer species.[23] The observed shifts near +37, +39, and −21 ppm for urohemin monomer and near +30, +33, +47, +48, and −34 ppm for the dimer are consistent with high-spin iron(III) porphyrin complexes and are not consistent with an antiferromagnetically coupled species.[23] The urohemin monomer is presumably an hydroxy complex. The dimer is either a π–π aggregate or a dihydroxy-bridged species as reported for other aqueous hemin solutions.[24]

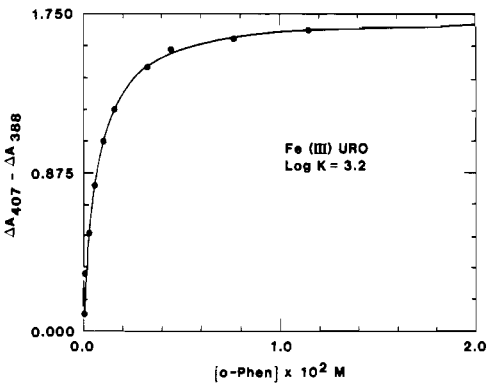

Figure 3. Plot of the difference in absorbance at 407 and 388 nm in the absorption difference spectra of the Soret band of FeURO in Figure 2. The curve is a least-squares fit of the theoretical 1:1 binding;

$$\text{FeURO} + \text{phen} \overset{K}{\rightleftharpoons} \text{FeURO–phen}$$

log K = 3.2. The temperature is 27 °C.

Equilibrium Binding Data. By far the most common pattern of shifts in absorption spectra is a red shift of all bands as illustrated by the phenanthroline complexes with FeURO (Figure 2). These spectral shifts provide a convenient means of determining the apparent equilibrium association constants K of these complexes by absorption difference spectroscopy. Figure 3 shows a plot of the difference in ΔA for the maximum at 407 nm and minimum at 388 nm (Figure 2) as a function

(17) Gouterman, M.; Stryer, L. *J .Chem. Phys.* **1962**, *37*, 2260.
(18) Brown, S. B.; Dean, T. C.; Jones, P. *Biochem. J.* **1970**, *117*, 733.
(19) Brown, S. B.; Hatzikonstantinou, H. *Biochem. Biophys. Acta* **1979**, *585*, 143.
(20) Blaner, G.; Zvilichovsky, B. *Arch. Biochem. Biophys.* **1968**, *127*, 749.
(21) Satterlee, J. D.; Shelnutt, J. A., in preparation.
(22) Shelnutt, J. A.; Dobry, M. M.; Satterlee, J. D., in preparation.
(23) LaMar, G. N.; Walker, F. A. In "The Porphyrins"; Academic Press: New York, 1979; Vol. IV, Part B, Chapter 2.
(24) Goff, H.; Morgan, L. O. *Inorg. Chem.* **1976**, *15*, 2062.

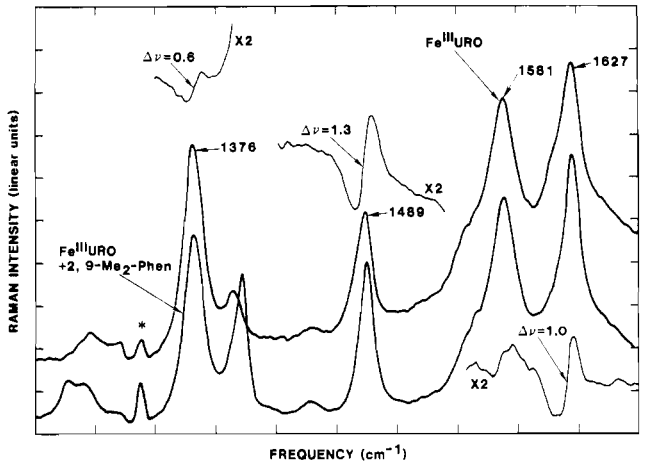

Figure 4. Raman spectrum of FeURO, the 2,9-Me_2phen–FeURO complex, and the Raman difference spectra. The RDS are expanded by a factor of 2. The calculated frequency shifts are indicated. A Raman line of 2,9-Me_2phen is observed near the FeURO line at 1402 cm^{-1}. The peak marked with an asterisk is an emission line (488 nm) of the laser. Instrumental parameters for the spectra are described in the text.

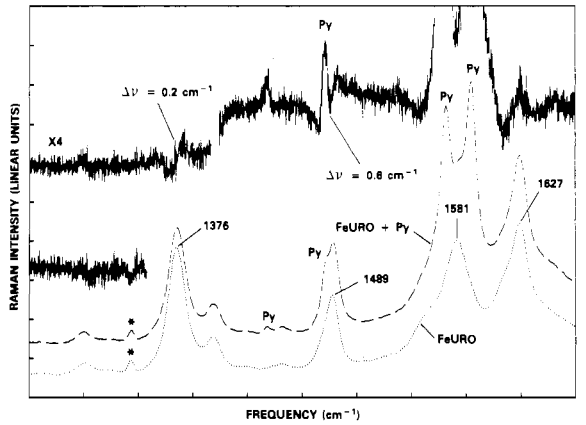

Figure 5. Raman spectrum of the pyridine complex with FeURO (---), the spectrum of FeURO alone (···), and the Raman difference spectrum (×4). The pyridine concentration is high (>0.1 M); therefore, several pyridine lines are superimposed on the FeURO spectrum (marked py). The calculated, complex-induced shifts are indicated for ν_4 and ν_3.

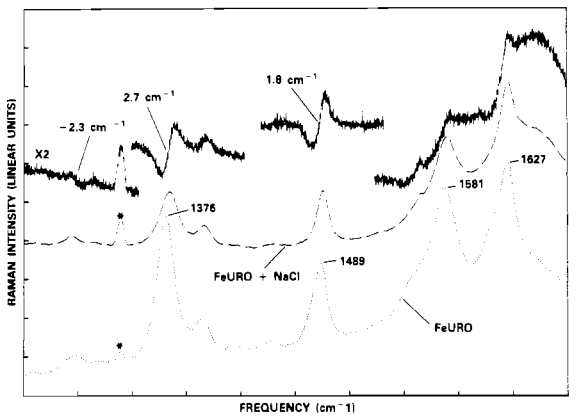

Figure 6. Raman spectrum of FeURO in an aggregated state at 3 M NaCl in 0.1 M NaOH (---), the Raman spectrum of FeURO in the absence of salt (···), and the Raman difference spectra (×2). The asterisk designates a laser emission line at 1345 cm^{-1}.

of the total concentration of phenanthroline. The line through the data points is a theoretical curve obtained by a simple 1:1 equilibrium binding analysis. A good least-squares fit was obtained with an equilibrium association constant of about 1600 (log K = 3.2). For the highest concentration of phenanthroline (near saturation in H_2O), the curve shows that complex formation is about 95% complete. By contrast, neocuproine was about 76% complexed at saturation (2×10^{-3} M 2,9-Me_2phen), and a least-squares fit was obtained for a log K of 3.3. Frequency shifts in the Raman lines reported in Table II have been corrected for incomplete complex formation.

Table I gives the equilibrium binding data for complexes of metallouroporphyrins with the addends listed in the first column. For the phen–CuURO complexes, the binding energies at 27 °C in 0.1 M NaOH range from 2.8 kcal/mol (5,6-phen-dione) to 6.2 kcal/mol (5-Cl-phen).

The data in Table I clearly indicate that the metal in the porphyrin has little influence on phenanthroline binding. For example, for the 1,10-phen and 2,9-Me_2phen complexes in 0.1 M NaOH, the binding energies for iron and copper porphyrins do not differ by more than 0.9 kcal/mol. In contrast, a comparison of either copper or iron porphyrin to the free base shows a small but significant reduction in the binding energy of about 0.9–1.8 kcal/mol (e.g., compare ΔG for the phen–FeURO (4.4 kcal/mol) and the phen–H_2URO (3.5 kcal/mol) complexes). However, the phenanthrolines still bind strongly to uroporphyrin even when no metal is present.

From Table I one can also see that the position of the nitrogen atoms in the phenanthroline ring only marginally ($\lesssim$0.5 kcal/mol) affects the binding energy in 0.1 M NaOH solutions. This is revealed by comparing free energies for the complexes of 1,10-phen (5.3 kcal/mol), 1,7-phen (5.8 kcal/mol), and 4,7-phen (5.8 kcal/mol) with CuURO.

Finally, steric hindrance of the lone-pair orbitals of the nitrogens of the phenanthrolines does not affect binding significantly as shown by a comparison of ΔG for the hindered 2,9-Me_2phen complex (Figure 8) and the less hindered 1,10-phen complex for both copper and iron uroporphyrins.

For comparison with the phenanthroline complexes, I have included in Table I the equilibrium association data for complexes with methylviologen (MV^{2+}), chloroquine (CQ^{2+}), pyridine, and 2,6-lutidine. The methylviologen dication is seen to bind more tightly than phenanthroline and its derivatives and isomers. The antimalarial drug chloroquine also exists as a cation at pH 8.4 and exhibits strong binding to the negatively charged porphyrin. Pyridine, on the other hand, binds more weakly than the phenanthroline derivatives and the cations (ΔG = 0.8 kcal/mol for H_2URO).

Raman Spectra and Spectral Shifts. The metal coordinated in the uroporphyrin core affects the frequencies of the Raman lines of the uncomplexed metalloporphyrins as shown in Table II. The lines at 1379 (ν_4), 1499 (ν_3), and 1637 cm^{-1} (ν_{10}) for CuURO are shifted to 1376 (−3 cm^{-1}), 1489 (−11 cm^{-1}), and 1627 cm^{-1} (−10 cm^{-1}) for FeURO and to 1383 (+4 cm^{-1}), 1518 (+19 cm^{-1}), and 1656 (cm^{-1} (+18 cm^{-1}) for NiURO. Therefore, this group of lines (ν_4, ν_3, and ν_{10}) shifts as a group when the metal is varied, and the frequencies follow the order Ni > Cu > Fe(III). The shift in the oxidation-state marker line ν_4 is about one-third of the shifts in the other two lines for Fe(III) → Cu(II) and about one-fifth of the shifts in the other two lines for Cu(II) → Ni(II) substitution.

Typical resonance Raman and Raman difference spectra for several complexes are shown in Figures 4–6. The Raman lines are generally those associated with in-plane vibrations of the porphyrin ring. The Raman lines of the porphyrin dominate the spectrum, even though the concentration of the porphyrin is roughly 1–3 orders of magnitude lower than the complexing addend, because of resonance enhancement of Raman scattering from the porphyrin. Resonance enhancement occurs because the frequency of the laser light that

Table II. Metalloporphyrin Raman Line Frequencies and Shifts[a] upon Formation of Complex with Phenanthroline and Methylviologen in 0.1 M NaOH (and in Aqueous Alkaline MeOH) (cm^{-1})

CuURO			NiURO			$Fe^{III}URO$			CoURO		
ν	$\Delta\nu_{phen}$[c]	$\Delta\nu_{MV^{2+}}$[d]	ν	$\Delta\nu_{phen}$[b]	$\Delta\nu_{MV^{2+}}$[d]	ν	$\Delta\nu_{phen}$[b]	$\Delta\nu_{MV^{2+}}$[d]	ν	$\Delta\nu_{phen}$[b]	$\Delta\nu_{MV^{2+}}$[d]
752	−0.2										
970	1.3										
995	>0										
1065	>0										
1102	−1.2	−2.7									
1131	1.2										
1161	0.5	−2.0									
1245	−1.8										
1310	0.2 (0.8)		1300	1.4	−0.2	1307			1309	−0.4	
1379	0.4 (0.5)	−2.4	1383	0.4	−2.0	1376	0.6	−2.9			
1403			1406		−3.0	1402			1402	>0	
1499	1.9	−2.2	1518	2.9	−5.2	1489	2.0		1510	4.0	
1582	>0 (1.2)	−4.3	1602	2.8	−8.8	1581	>0	−2.4	1598	3.0	
1637	2.0 (1.7)	−1.3	1656	5.3[e]	−1.4	1627	2.0	−2.4	1647	4.4	

[a] Corrected for incomplete complex formation. [b] $f = 1.08$. [c] $f = 1.05$. [d] $f = 1.00$. [e] Large line width change.

excites the Raman spectrum is coincident with a $\pi \rightarrow \pi^*$ electronic transition of the porphyrin. In the present study, resonance enhancement permits selective excitation of the complexed metalloporphyrin without interference from either the complexed or the uncomplexed addend molecules, which are present at higher concentration than the porphyrin.

A unique feature of the present Raman study is the use of the Raman difference apparatus.[5,9,14,25-27] With this instrument the spectra of two distinct molecules (in the present case, the porphyrin and the porphyrin–addend complex) can be obtained simultaneously. The RDS technique allows accurate comparisons of the frequencies, shapes, and intensities of the Raman lines of the porphyrin and the complex. Differences in frequency $\Delta\nu$ of the Raman lines of the metalloporphyrin alone and in the presence of addend can easily be obtained to an accuracy of 0.1 cm^{-1}. The differences reported are calculated from the approximate formula[27] $\Delta\nu = 0.38 f I_d \Gamma / I_o$, where Γ is the line width at half-maximum and I_o is the intensity of the line as measured from the Raman spectrum. I_d is the peak-to-valley intensity of the deflection in the difference spectrum that occurs for lines of the metalloporphyrin–addend complex that are shifted with respect to those of the metalloporphyrin; f is a correction factor equal to 1 over the fraction of metalloporphyrin molecules that have complexed with addend. If the shift is larger than half the line width or if the shape of the Raman line of the complex is different from that of the metalloporphyrin, then the formula gives an inaccurate value for $\Delta\nu$. In the former case, a more complicated expression must be used to calculate $\Delta\nu$.[26,27] Sometimes, in the latter case, the number derived from the formula is a useful measure of the differences in the Raman spectra even though it should not be thought of purely as a frequency shift.

Figure 4 shows the Raman spectra of FeURO (7×10^{-5} M) and the 2,9-Me_2phen–FeURO complex along with the Raman difference spectrum of each line. Clear differences in frequency are noted in the ν_4, ν_3, ν_{19} (1581 cm^{-1}), and ν_{10} vibrations. From the above formula, the differences are calculated to be +0.6, +1.3, +1.0, and +1.0 cm^{-1}, respectively. The calculated shifts may have larger than usual errors for the three highest frequency lines since line-shape changes occur upon complex formation for these Raman lines. The small shape change was ignored in calculating the line shift.

Figure 5 shows the Raman difference data for the pyridine complex. Note again clear shifts in the same lines that are shifted for the phenanthroline complexes. The pattern of shifts for pyridine is also similar to that of the phen complexes with ν_4 showing smaller shifts than ν_3 and ν_{10}.

Table III. Frequency Shifts in Raman Marker Lines for Iron(III) Uroporphyrin Complexes with Derivatives of Phenanthroline in 0.1 M NaOH

	shifts			
addend	1376 cm^{-1}	1489 cm^{-1} [a]	1581 cm^{-1}	1627 cm^{-1} [a]
1,10-phen	0.6	1.8	>0	1.8
4,7-phen	>0	2.2	>0	2.2
1,7-phen				2.2
2,9-Me_2phen	0.6	1.3	1.0	1.0
4,7-Me_2phen	2.2[b]	1.3	>0	1.1
5,6-Me_2phen		1.2	>0	1.1
4-Me-phen		1.9	2.3	1.2
5-Me-phen	b	1.8	1.7	1.5
5-Cl-phen	0.7	2.1	1.9	1.9

[a] Line shape change. [b] Obscuring phen line.

Finally, in Figure 6 the Raman difference data for salt-aggregated FeURO is presented. Frequency shifts of about 2 cm^{-1} to higher frequency are found for all high-frequency Raman lines except the 1307-cm^{-1} line, which shifts to lower frequency for the aggregate. Thus, the pattern of Raman line shifts for aggregated FeURO at high salt concentrations is different from that for complex formation with neutral addends such as phenanthroline.

The shifts calculated from the Raman difference spectra for complexes of phenanthroline and methylviologen with CuURO, NiURO, CoURO, and FeURO are compared in Table II. First, independent of the metal in the porphyrin, most of the Raman lines, in particular the high-frequency lines, shift to higher frequency for 1,10-phen complexes; they shift to lower frequency for methylviologen dication complexes. Further, the pattern of shifts upon complexation is distinct for the two addends. For phen complexes the shift in ν_4 is much smaller than the shifts in ν_3 and ν_{10}. In contrast, for the MV^{2+} complexes the shifts in all of these lines are of about equal magnitudes.

For phen complexes the ratio of the shift in ν_4 to the shift in either ν_3 or ν_{10} depends on the metal. For CuURO this ratio is about 1:5. For NiURO and CoURO the ratio is smaller (1:7 to 1:12), and for FeURO it is larger (1:3). It is interesting that the ratio of the complex-induced shifts for the different metals reflects to some degree the ratio of the metal-dependent shifts in these lines that was noted above after substitution of Ni (1:5) or Fe (1:3) for Cu in the uroporphyrin.

Table III gives the shifts in ν_4, ν_3, ν_{19}, and ν_{10} for complexes of FeURO with some derivatives and isomers of phenanthroline. All of the shifts are to higher frequency. Although

(25) Shelnutt, J. A.; Rousseau, D. L.; Dethmers, J. K.; Margoliash, E. *Biochemistry* **1981**, *20*, 6485.
(26) Rousseau, D. L. *J. Raman Spectrosc.* **1981**, *10*, 94.
(27) Kiefer, W. *Appl. Spectrosc.* **1973**, *27*, 253.

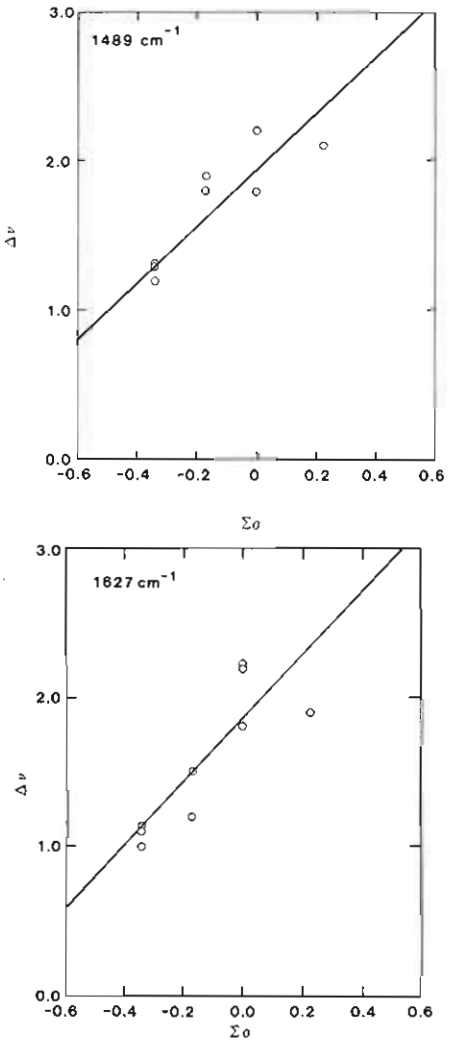

Figure 7. Correlation between the complex-induced shift in the 1489- (ν_3) and 1627-cm^{-1} (ν_{10}) Raman lines and the sum of the Hammett constants of the substituents on the phenanthroline ring. The para substituent constants have been used. The correlation coefficients are 0.85 (ν_{10}) and 0.87 (ν_3).

the possible errors are somewhat larger than those for the corresponding CuURO data,[8,9] the results are similar.

Figure 7 shows the linear relationship between the complex-induced shifts in ν_{10} and ν_3 for FeURO–phen complexes and the Hammett constants[28] for the phenanthroline substituents. A clear correlation is observed for FeURO complexes, although the scatter in the data is somewhat greater than that of CuURO complexes.[8,9]

From the equilibrium binding data for the CuURO–phen complexes, the degree of complex formation can be estimated to vary between 73% (5,6-phen-dione) and 93% (e.g., 1,7-phen) except for phenyl derivatives; the average is 85%. Therefore, almost all of the shifts reported are roughly 15% smaller than the actual shifts for the complex, and the relative errors are less than 10%. This is less than errors in measurements of frequency shifts, so the data in Table III and Figure 7 have not been corrected for incomplete complex formation.

Discussion

The most obvious conclusions that can be derived from the results presented above are (1) that the copper and iron(III) uroporphyrins form very similar complexes with phenanthrolines, methylviologen dication, and pyridines and (2) that interactions between the nitrogen lone pairs and the metal are relatively unimportant. The evidence is outlined below.

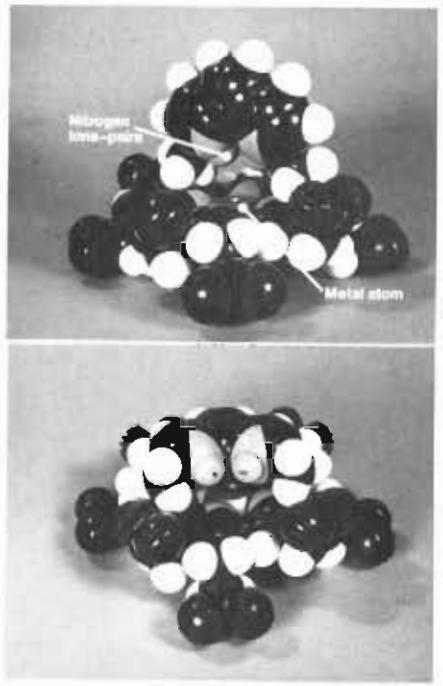

Figure 8. Top: Molecular model of a hypothetical "perpendicular" orientation of the rings in the 2,9-Me$_2$phen–metallouroporphyrin complex. Note the two methyl groups prevent interaction of the nitrogen lone pairs with an in-plane metal ion. Bottom: Illustration of a possible "parallel" ring orientation for the $\pi-\pi$ complex (see Table III).

First, equilibrium data in Table I show that binding energies for the phenanthrolines are remarkably insensitive to the metal incorporated into the porphyrin and that they are only slightly affected even by the absence of the central metal ion. As seen in Figure 8 (top), 2,9-Me$_2$phen has highly sterically hindered lone pairs on the nitrogens, so that axial ligation at the metal is forbidden if the metal is in plane as is the case for CuURO. The metal may be out of plane in iron(III) uroporphyrin, and, consequently, a strong interaction between Fe(III) and the 2,9-Me$_2$phen derivative might have been expected. However, this is not reflected in the binding energies, since they are identical for the iron(III) and copper porphyrins (4.5 kcal/mol). As noted previously,[8,9] for CuURO the binding energy of the 2,9-Me$_2$ derivative is not significantly lower than that of the unhindered dimethyl derivatives.

The pyridines behave in a similar manner. The nature of the metal present, even the absence of the metal ion, only weakly affects the binding energy of pyridine (Table I). Furthermore, for the in-plane copper porphyrin, steric hindrance of the nitrogen lone pair does not lower the binding energy for 2,6-lutidine as would be expected if interaction of the lone pair with the metal were important.

The changes in the absorption spectra of complexes with iron and copper porphyrins are also similar, although the FeURO spectrum itself is more complex than that of CuURO. Red shifts of both the Soret and visible bands occur upon binding of phenanthroline to either the copper or the iron porphyrin. For the complex of methylviologen with FeURO, a blue shift of the α band and a red shift of the Soret is observed (Figure 1); similar shifts occur upon formation of the CuURO–MV^{2+} complex. However, upon complexation with imidazole, the absorption spectrum of FeURO changes entirely, reflecting binding at the iron ion and the change from the high- to low-spin state (Figure 1).

Finally, changes in the Raman spectra that accompany complex formation are similar for FeURO and CuURO. For both metalloporphyrins, the Raman lines at high frequency

(28) McDaniel, D. H.; Brown, H. C. *J. Org. Chem.* **1958**, *23*, 420.

shift to higher frequency by several wavenumbers upon complexation with phenanthroline. Also, the shift in the pure oxidation state marker line ν_4 is smaller than it is for ν_3, ν_{19}, and ν_{10} regardless of the metal present. This pattern of shifts is preserved for the pyridine complex as shown by Figure 5.

The positions of the nitrogen atoms in the phenanthroline ring have little effect on the Raman shifts for the complexes (Table III and Figure 7) regardless of the metal present in the porphyrin ring. Also, the binding affinities of the phenanthroline isomers differ little, further suggesting that direct interaction of the metal with the nitrogen lone pairs is relatively unimportant.

The Raman results, in particular, further suggest that the phenanthroline complexes are π–π complexes. Derivatives of phenanthroline produce shifts in the CuURO Raman lines that correlate with the acceptor abilities and the binding energies of the derivatives.[8,9] Derivatives of phenanthroline that are hindered from lying flat on the porphyrin ring do not correlate with acceptor ability, which suggests that a π–π interaction is involved in the formation of CuURO complexes. The correlations also suggest that a charge-transfer component of the intermolecular interaction is important. Correlations between Hammett constants and molecular structural properties, such as vibrational frequencies, are often observed for a series of related π acceptors with a given donor.[29]

As shown in Figure 7, the ν_3 and ν_{10} vibrations of FeURO also correlate with the sum of the Hammett constants of the substituents on the phenanthroline ring. Therefore, this relationship holds for complexes with both CuURO and FeURO and further provides evidence for a π–π charge-transfer contribution to the forces stabilizing the FeURO–phen complexes. However, a high-fluorescence background for hindered complexes has so far prevented verification that FeURO–phen complexes are destabilized for phenanthrolines that cannot lie flat on the macrocycle.

The relationship between $\Delta\nu$ and the acceptor ability of the addend accounts for the small shifts of the complexes of 2,9-dimethylphenanthroline with CuURO and FeURO. The electron-donating properties of the metal substituents of 2,9-Me_2phen (and 5,6-Me_2phen and 4,7-Me_2phen) reduce its acceptor ability, and this reduction explains the smaller Raman frequency shifts associated with formation of dimethylphenanthroline complexes. Thus, steric hindrance of the lone pairs is not a factor.

Metal Effects on Porphyrin Electronic Structure. In order to make a more complete assessment of the effects of complex formation on the metalloporphyrin, the causes of the shifts in the Raman lines must be understood in some detail. In particular, the similarity of the changes in the Raman lines when either the metal is changed or phenanthroline is bound suggests that a common property of the porphyrin is influenced by these two dissimilar phenomena. Since many vibrational modes of the ring are affected, searching for a common *electronic* structural change in the π system of the macrocycle is most productive.

Fortunately, several Raman lines are sensitive to the electron density of the frontier orbitals of the porphyrin ring but are insensitive to perturbations by peripheral substituents.[30-33] The ν_4 vibration, for example, is a well-known pure oxidation-state marker line because it shifts to higher frequency as the oxidation state of the metal increases, but it is insensitive to the spin state of the metal.[30] For iron porphyrins this relationship holds for the 2+, 3+, and 4+ oxidation states.[30-33] The ν_3, ν_{19}, and ν_{10} vibrational frequencies also increase with the increasing oxidation state but are affected by spin state as well.[30] Increasing the valence of the metal decreases back-bonding to the antibonding $e_g(\pi^*)$ orbital of the porphyrin ring, thereby raising the frequencies of these and other Raman lines. The ν_4 vibration is also sensitive to the oxidation state of the ring for the π mono- and dianions of vanadyl and zinc porphyrins.[34] Molecular orbital calculations predict that electron(s) will enter the frontier $e_g(\pi^*)$ orbital in these anions.[35] Therefore, the π-anion data are consistent with the hypothesis that ν_4 is a marker of the charge density in the $e_g(\pi^*)$ orbital of the ring. However, spectra of vanadyletioporphyrin dication also show a shift of 9 cm^{-1} to lower frequency relative to the frequency of ν_4 for the neutral molecule;[36] thus, ν_4 may be dependent on bonding orbitals as well.

Through interaction with σ and π donors and acceptors at the fifth and sixth ligand sites, the iron d_π orbitals become either better donors or better acceptors with respect to the $e_g(\pi^*)$ orbitals of the porphyrin ring. The frequencies of several lines, including ν_4, increase with decreasing $e_g(\pi^*)$ charge density for a series of π-acid bis ligands.[37] (See also ref 9 and 10.)

In contrast, ν_3, ν_{19}, and ν_{10} must be more sensitive to other orbital populations since they also depend on the spin state of the iron.[30] Further, these three lines are well-characterized structural markers of the size of the central core of the porphyrin ring.[38] Theoretical considerations suggest that the metal dependence of these lines is caused by changes in electron density within the macrocycle, however, rather than by mixing with the metal–nitrogen vibrations.[39]

Kitagawa[40] has pointed out that variations in the frequencies of these lines follow the electronegativity of the metal for the H_2, Zn, Cu, Co, and Ni series of octaethylporphyrins.[14] Other workers[13-15,41,42] had noted previously that the electronegativity E_N of the metal influences the conjugation of the metal to the porphyrin. Gouterman[15] has suggested that increased conjugation lowers the $a_{2u}(\pi)$ orbital by interaction with an empty p_z metal orbital. The lowered energy and charge of the $a_{2u}(\pi)$ orbital decrease the porphyrin bond energies and would likely increase some force constants. The $a_{2u}(\pi)$ orbital density is mainly on the meso carbon atoms and the pyrrole nitrogens. Since a normal coordinate analysis of the porphyrin shows that the three core-size marker lines are predominately C_m–C_α stretching,[43] it is not surprising that they would reflect stabilization of the $a_{2u}(\pi)$ orbital. Kitagawa[40] has observed that the frequency of the α-band absorption ν_α is proportional to the frequencies of the core-size marker lines for the stated series of metals, and he invoked Gouterman's argument to explain the result.

The wavelength of the α band has long been known to predict the stability of metalloporphyrins to demetalation by protic acids.[13,41,42,44-46] The shorter the wavelength, the more

(29) Foster, R. "Organic Charge-Transfer Complexes"; Academic Press: London, 1969.
(30) Spiro, T. G.; Strekas, T. C. *J. Am. Chem. Soc.* **1974**, *96*, 338.
(31) Rakhit, G.; Spiro, T. G.; Uyeda, M. *Biochem. Biophys. Res. Commun.* **1976**, *71*, 803.
(32) Sievers, G.; Osterlund, K.; Ellfolk, N. *Biochim. Biophys. Acta* **1979**, *581*, 1.
(33) Choi, S.; Spiro, T. G.; Langry, K. C.; Smith, K. M.; Budd, D. L.; LaMar, G. N. *J. Am. Chem. Soc.* **1982**, *104*, 4345.
(34) Ksenofontova, N. M.; Maslov, V. G.; Sidorov, A. N.; Bobovich, Ya. S. *Opt. Spectrosc. (Engl. Transl.)* **1976**, *40*, 462.
(35) Zerner, M.; Gouterman, M. *Theor. Chim. Acta* **1966**, *4*, 44.
(36) Aleksandrov, I. V.; Yeletskii, N. P.; Sidorov, A. N. *Biofizika* **1980**, *25*, 379 (*Biophysics (Engl. Transl.)* **1981**, *25*, 389).
(37) Spiro, T. G.; Burke, J. M. *J. Am. Chem. Soc.* **1976**, *98*, 5482.
(38) Spaulding, L. D.; Chang, C. C.; Yu, N.-T.; Felton, R. H. *J. Am. Chem. Soc.* **1975**, *97*, 2517.
(39) Gladkov, L. L.; Solov'ev, K. N. *Teor. Eksp. Khim.* **1980**, *16*, 705.
(40) Kitagawa, T.; Ogoshi, H.; Watanabe, E.; Yoshida, Z. *J. Phys. Chem.* **1975**, *79*, 2629.
(41) Anderson, J. S.; Bradbrook, E. F.; Cook, A. H.; Linstead, R. P. *J. Chem. Soc.* **1938**, 1151.
(42) Williams, R. J. P. *Chem. Rev.* **1956**, *56*, 299.
(43) Abe, M.; Kitagawa, T.; Kyogoku, Y. *J. Chem. Phys.* **1978**, *69*, 4526.
(44) Caughey, W.; Corwin, A. *J. Am. Chem. Soc.* **1955**, *77*, 1509.

stable is the metal–porphyrin bond. Recently, Buchler[47] has defined a stability index for the metal–porphyrin interaction given by ZE_N/r_i, where Z/r_i is a measure of the ionic part of the interaction and the electronegativity E_N measures the covalent part. This index predicts the stability of a wide variety of metalloporphyrins. Shelnutt[10] has recently shown that the core-size marker lines roughly correlate with the stability index for a series of metal uroporphyrins and octaethylporphyrins. The correlation is especially remarkable because the influence of out-of-plane distance and axial ligands of the metal was not considered.

The spin-state dependence of the core-size marker lines for the *iron porphyrins* can also be explained in terms of the associated changes in electronegativity and ionic radius of the metal and their influence on the $a_{2u}(\pi)$ orbital. High-spin Fe(II) has the lowest E_N (1.7)[48] and largest ionic radius (0.77 Å)[49] and hence the lowest value for the stability index. As predicted by the correlation, the core-size marker lines have the lowest frequencies (about 1554 (ν_{19}) and 1605 cm^{-1} (ν_{10})).[37] On the other hand, low-spin Fe(III) has the smallest ionic radius (0.55 Å)[49] and highest E_N (1.8)[48] and thus the highest stability. The core-size (or spin-state) marker lines attain their highest frequencies (about 1586 and 1642 cm^{-1})[37] in low-spin Fe(III) porphyrins. In fact, the stability indices of the iron porphyrins in all spin and oxidation states correlate reasonably well with the frequencies of the core-size marker lines. Further, the slope of the linear relationship between stability and Raman frequencies is about the same as for other metalloporphyrins.[10] This interpretation explains why the core-size marker lines are also spin-state marker lines and, moreover, lends some credence to arguments concerning charge density and stabilization of the $a_{2u}(\pi)$ orbital upon metal substitution.

Effect of Phenanthroline Complexation on Porphyrin Structure. With this background we can now offer an explanation of the Raman line shifts that occur upon formation of metalloporphyrin–phenanthroline complexes. Remember that, just as when the metal ion is varied, the "$a_{2u}(\pi)$-sensitive" (core-size marker) lines are shifted more than the "$e_g(\pi^*)$-sensitive" (oxidation-state marker) line after complexes with phenanthrolines are formed. This similarity in the pattern of shifts suggests that phenanthroline interacts predominately with the $a_{2u}(\pi)$ orbital. Further, the shifts in the $a_{2u}(\pi)$-sensitive Raman lines are *increases* in frequency, so that the $a_{2u}(\pi)$ orbital is stabilized and loses charge density. Therefore, phen is an acceptor of π density primarily from the highest filled $a_{2u}(\pi)$ orbital. The correlation of shifts in the $a_{2u}(\pi)$-sensitive lines with the acceptor properties of phen derivatives supports this hypothesis. Lack of a similar correlation for the oxidation-state marker line may be the result of the lack of significant π density in $e_g(\pi^*)$ for these metalloporphyrins.[10,35]

Another feature of the pattern of Raman line shifts for metalloporphyrin–phen complexes is that complexes with the porphyrins containing the most stable metals (Ni and Co) exhibit larger shifts in the core-size marker lines than those containing the least stable metals ($Fe^{III}OH$, Cu). In terms of the porphyrin structure, those metalloporphyrins with the *smallest* core size show the *largest reduction* in core size when phen binds.

The similarity of the effects of phen binding and metal substitution on the Raman line shifts may appear to imply that phen binds at the metal and in some way affects the porphyrin moiety through its influence on the metal. Strong binding to H_2URO and other results discussed above suggest, however, that the metal may not be the site of phen interaction. Furthermore, even though the Raman shifts associated with the two phenomena are similar, the electronic structure of the porphyrin is not identically affected.

An important distinction between the metal-dependent spectral shifts and the phen-induced shifts should be emphasized. The bathochromic shifts in the α band that accompany metal substitution are associated with shifts to *lower* frequencies for the core-size marker lines. This relationship holds for the present Raman data and was also noted by Kitagawa et al.[40] In contrast, the bathochromic shifts in the α band that occur upon phen binding are accompanied by shifts to *higher* Raman frequencies. Therefore, for the phen-induced shifts the proportionality between ν_α and the frequencies of the core-size marker lines no longer holds. This lack of proportionality suggests that orbitals other than the $a_{2u}(\pi)$ orbital, and that by symmetry cannot conjugate with the metal p_z orbital, are involved in the interaction with phen. For example, the $a_{1u}(\pi)$ orbital has a node at the pyrrole nitrogens and, hence, cannot be affected by the metal–nitrogen interaction but can be influenced by interaction with phen. The $e_g(\pi^*)$ orbital may also be influenced by phen binding but not by conjugation with the p_z orbital. Thus, ν_α depends on excited-state energies that might be influenced by phen as well as the ground-state energy, but the Raman frequencies depend only on the ground state of the molecule.

Induction effects of the metal also influence the spectra. A decrease in the σ-electron density on the pyrrole nitrogens alters the Coulomb integral, unequally lowering the energy of the $e_g(\pi^*)$ and $a_{2u}(\pi)$ orbitals. Therefore, inductive effects can cause a shift in the transition energy and can influence the Raman spectrum as well.

Structure of the Phenanthroline Complex. All of the above data are consistent with a $\pi-\pi$ interaction between the stacked ring systems of phen and the metalloporphyrin macrocycle. As can be seen in Figure 8 (bottom), the uroporphyrin molecule can easily accommodate either one or two phen molecules (above and below the porphyrin ring). The equilibrium binding data indicate that complexes of CuURO with phenanthrolines having strong acceptor properties are best described by strong binding of one molecule of phen and subsequent weaker binding of a second phen molecule (K about a factor of 10 smaller). However, phenanthrolines with weak acceptor ability appear to bind in a 1:1 fashion. 1,10-phen binds to CuURO in a 2:1 complex.

In contrast, the equilibrium data for binding of 1,10-phen to FeURO is adequately described by a 1:1 binding analysis, as can be seen in Figure 3. Binding of phen to one side of the porphyrin ring may be blocked by an OH^- counterion in the case of the Fe^{III}URO complex. Vanadyluroporphyrin also has one side of the ring blocked by the strongly bound vanadyl oxygen and only binds one phen.[50] The low-spin dicyanide–FeURO complex, in which both axial ligand sites are occupied, appears not to bind phenanthroline at all; therefore, strong axial ligation may block $\pi-\pi$ complex formation.

The orientation of the phen ring with repect to the metalloporphyrin cannot be determined from the present work. However, the distribution of total π charge[51] in the free-base porphyrin suggests that the phen ring is preferred by the two pyrroles with protons attached. These pyrroles have high π charges, particularly on the nitrogens, and would make good donors. The proposed orientation of phen is consistent with

(45) Falk, J. "Porphyrins and Metalloporphyrins"; Elsevier: Amsterdam, 1964.
(46) Fisher, M. S.; Weiss, C. *J. Chem. Phys.* **1970**, *53*, 3121.
(47) Buchler, J. W.; Puppe, L.; Rohbock, K.; Schneehage, H. H. *Ann. N.Y. Acad. Sci.* **1973**, *206*, 116.
(48) Gordy, W.; Thomas, W. J. O. *J. Chem. Phys.* **1956**, *24*, 439.
(49) Shannon, R. D.; Prewitt, C. T. *Acta Crystallogr., Sect. B* **1969**, *B25*, 925.
(50) Shelnutt, J. A.; Dobry, M. M. *J. Phys. Chem.*, in press.
(51) Petke, J. D.; Maggiora, G. M.; Shipman, L. L.; Christoffersen, R. E. *J. Mol. Spectrosc.* **1978**, *71*, 64.

larger shifts in the x-polarized absorption bands than in the *y*-polarized bands for the free-base complex.

Solvent Effects on Phenanthroline Binding. Comparisons of binding affinities of phenanthroline–metalloporphyrin complexes in alkaline H_2O and in aqueous alkaline methanol indicate that the solvent has a large effect on affinity. In the organic, relatively less structured solvent methanol, the binding energy is always reduced, and for some derivatives it is reduced by more than one-half (Table I). Weak binding may reflect a large entropic destabilization in methanol in which phen is highly soluble.

It is useful to compare the enthalpy and entropy of a typical charge-transfer complex with that of the phen–metalloporphyrin complex. For example, the donor hexamethylbenzene (HMB) forms a charge-transfer complex with a strong acceptor such as trinitrobenzene (TNB). The HMB–TNB complex has a $-\Delta H$ of 3.7 kcal/mol and a $-\Delta S$ of 8.8 cal/(K mol).[29] For the 2,9-Me_2phen–CuURO complex one finds that $-\Delta H$ = 6.4 kcal/mol and $-\Delta S$ = 6.7 cal/(K mol) (when a 1:1 binding analysis is used). The remarkable stability of the phen complex appears to result from both a large enthalpy of formation and a low entropic term. The entropy effect probably dominates. Indeed, for the highly soluble 4,7-$(OH)_2$phen derivative, $-\Delta H$ = 5.6 kcal/mol is somewhat smaller and $-\Delta S$ = 8.2 cal/(K mol) is considerably larger than for the 2,9-Me_2phen complex. Consequently, the stability of the phen-diol complex is much lower.

Aqueous Pyridine–Metalloporphyrin Complexes. Some evidence in the present work suggests that pyridine binds as much to the porphyrin ring as to the metal in aqueous solvent as Mauzerall has suggested.[11] Of foremost importance is the lack of significant difference in the affinity of pyridine for H_2URO, CuURO, and FeURO. Also, neither the metal nor steric hindrance of the lone pair in 2,6-lutidine has any effect on affinity (Table I).

The Raman difference spectra (Figure 5) show that the pattern of shifts for the pyridine complex is similar to that of phenanthroline complexes with the shift of ν_4 smaller than that of ν_3 and ν_{10}. In addition, shifts in ν_3 and ν_{10} observed with 2,6-lutidine are larger than those of the unhindered py–FeURO complex (Figure 5).

Summary. The effect of the metal on the high-frequency vibrational spectrum of porphyrin can be explained in terms of its effect on the electronic structure of the macrocycle. Properties of the metal, such as electronegativity and ionic radius, influence conjugation of the metal with the π-electron system. Increased stability of the metal–porphyrin bond stabilizes the $a_{2u}(\pi)$ orbital, in particular. Reduced charge density in the $a_{2u}(\pi)$ orbital causes the C_m–C_α stretching vibrations (core-size marker lines) to increase in frequency.

Molecular complexes with neutral aromatic acceptors such as phenanthroline result in shifts in the Raman lines that are similar to those associated with metal substitution. The $\pi \rightarrow \pi^*$ absorption bands also shift upon binding of phenanthroline. Similarities in the patterns of Raman line shifts suggest a connection between the effects of metal substitution and π–π complex formation. Charge transfer from the highest occupied orbitals of the porphyrin ring to phenanthroline accounts for the Raman results and provides the necessary association with metal effects on the $a_{2u}(\pi)$ orbital.

The data presented for urohemin–phenanthroline complexes support a charge-transfer interaction between the stacked ring systems. The Raman line shifts, absorption band shifts, and equilibrium binding constants for the FeURO–phen complexes are similar to those of other metalloporphyrin–phen complexes. Differences in these properties for urohemin are a consequence of the effect of the metal ion on the electronic structure of the ring.

Although the Raman shifts are small ($\sim$1 cm^{-1}), significant energy ($\gtrsim$1 kcal/mol)[9] is associated with the charge-transfer interaction. For molecules for which the vibrational–electronic coupling is weak, only small shifts are expected to be associated with substantial changes in electronic structure. That vibronic coupling is weak for natural metalloporphyrins is demonstrated by the success of the free-electron model of their electronic states[15,52] and of calculations of Raman excitation spectra.[53,54] These results suggest that the small Raman marker line shifts in heme proteins[5,6,14,25,55,56] may be energetically important.

The effects of complexation with aromatic cations are distinct from those of complexation with neutral aromatics. The differences are illustrated by the distinct patterns of shifts in the Raman lines for the viologen and chloroquine complexes and salt-induced aggregates.

Acknowledgment. I thank Mary Dobry for her technical assistance and Sieglinde Neuhauser for editorial assistance with the manuscript.

Registry No. 1,10-phen–CuURO, 78803-43-7; 1,10-phen–Fe(OH)URO, 84254-33-1; 1,10-phen–H_2URO, 86480-86-6; 1,10-phen–NiURO, 84254-31-9; 1,7-phen–CuURO, 78820-51-6; 4,7-phen–CuURO, 78803-44-8; 2,9-Me_2phen–CuURO, 78803-56-2; 2,9-Me_2phen–Fe(OH)URO, 86480-87-7; 4,7-Me_2phen–CuURO, 78803-57-3; 5,6-Me_2phen–CuURO, 78803-58-4; 4-Me-phen–CuURO, 78803-46-0; 5-Me-phen–CuURO, 78803-48-2; 5-Cl-phen–CuURO, 78803-50-6; 5-NO_2phen–CuURO, 78803-52-8; 5-Ph-phen–CuURO, 78803-54-0; 4,7-$(OH)_2$phen–CuURO, 78803-66-4; 5,6-phen-dione–CuURO, 78803-64-2; MV^{2+}–CuURO, 78991-91-0; pyridine–CuURO, 84098-88-4; pyridine–H_2URO, 86480-88-8; pyridine–Fe(OH)URO, 86480-89-9; 2,6-lutidine–CuURO, 86480-90-2; chloroquine–CuURO, 86480-92-4; chloroquine–Fe(OH)URO, 86480-93-5; 1,10-phen–CoURO, 84254-35-3; 4,7-phen–Fe(OH)URO, 86496-99-3; 1,7-phen–Fe(OH)URO, 86480-95-7; 4,7-Me_2phen–Fe(OH)URO, 86480-96-8; 5,6-Me_2phen–Fe(OH)URO, 86480-97-9; 4-Me-phen–Fe(OH)URO, 86480-98-0; 5-Me-phen–Fe(OH)URO, 86480-99-1; 5-Cl-phen–Fe(OH)URO, 86481-00-7; MV^{2+}–NiURO, 86481-02-9; MV^{2+}–Fe(OH)URO, 86497-01-0.

(52) Simpson, W. T. *J. Chem. Phys.* **1949**, *17*, 1218.
(53) Shelnutt, J. A. *J. Chem. Phys.* **1981**, *74*, 6644.
(54) Shelnutt, J. A.; O'Shea, D. C. *J. Chem. Phys.* **1978**, *69*, 5361.
(55) Ondrias, M. R; Rousseau, D. L.; Shelnutt, J. A.; Simon, S. R. *Biochemistry* **1982**, *21*, 3428.
(56) Rousseau, D. L.; Shelnutt, J. A.; Henry, E. R.; Simon, S. R. *Nature (London)* **1980**, *285*, 49.